An inducible helix–Gly–Gly–helix motif in the N-terminal domain of histone H1e: A CD and NMR study

ROGER VILA,[1] IMMA PONTE,[1] M. ANGELES JIMÉNEZ,[2] MANUEL RICO,[2] AND PEDRO SUAU[1]

[1]Departamento de Bioquímica y Biología Molecular, Facultad de Ciencias, Universidad Autónoma de Barcelona, E-08193 Bellaterra, Barcelona, Spain
[2]Instituto de Estructura de la Materia, CSIC, Serrano 119, E-28006 Madrid, Spain

(RECEIVED July 18, 2001; FINAL REVISION October 16, 2001; ACCEPTED October 24, 2001)

Abstract

Knowledge of the structural properties of linker histones is important to the understanding of their role in higher-order chromatin structure and gene regulation. Here we study the conformational properties of the peptide Ac-EKTPVKKKARKAAGGAKRKTSG-NH_2 (NE-1) by circular dichroism and ^{1}H-NMR. This peptide corresponds to the positively charged region of the N-terminal domain, adjacent to the globular domain, of mouse histone H1e (residues 15–36). This is the most abundant H1 subtype in many kinds of mammalian somatic cells. NE-1 is mainly unstructured in aqueous solution, but in the presence of the secondary-structure stabilizer trifluoroethanol (TFE) it acquires an α-helical structure. In 90% TFE solution the α-helical population is ~40%. In these conditions, NE-1 is structured in two α-helices that comprise almost all the peptide, namely, from Thr17 to Ala27 and from Gly29 to Thr34. Both helical regions are highly amphipathic, with the basic residues on one face of the helix and the apolar ones on the other. The two helical elements are separated by a Gly–Gly motif. Gly–Gly motifs at equivalent positions are found in many vertebrate H1 subtypes. Structure calculations show that the Gly–Gly motif behaves as a flexible linker between the helical regions. The wide range of relative orientations of the helical axes allowed by the Gly–Gly motif may facilitate the tracking of the phosphate backbone by the helical elements or the simultaneous binding of two nonconsecutive DNA segments in chromatin.

Keywords: Histone H1; N-terminal domain; amphipathic helix; helix–Gly–Gly–helix motif; circular dichroism; nuclear magnetic resonance

Supplemental material: See www.proteinscience.org.

The linker histone H1 has a central role in stabilizing both the nucleosome and chromatin higher-order structure. H1 histones have a characteristic three-domain structure (Hartman et al. 1977). The central globular domain consists of a three-helix bundle with a β-hairpin at the C terminus (Clore et al. 1987; Cerf et al. 1993; Ramakrishnan et al. 1993) that is similar to the winged-helix motif found in some sequence-specific DNA-binding proteins. The N terminus and the C terminus are highly basic. The terminal domains have, in general, little structure in solution. The C-terminal domain acquires, however, a substantial amount of α-helical structure in the presence of secondary-structure stabilizers such as trifluoroethanol (TFE) or $NaClO_4$ (Clark et al. 1988; Hill et al. 1989). A turn and a helix–turn motif in the C-terminal domain have been characterized by high-resolution NMR in the presence of structure stabilizers (Suzuki et al. 1993; Vila et al. 2000). It has also been shown that a peptide

Reprint requests to: Dr. Pedro Suau, Departamento de Bioquímica y Biología Molecular, Facultad de Ciencias, Universidad Autónoma de Barcelona, E-08193 Bellaterra, Barcelona, Spain; e-mail: Pere.Suau@uab.es; fax: 34-935811264.

Article and publication are at http://www.proteinscience.org/cgi/doi/10.1110/ps.29602.

belonging to the C-terminal domain of H1° acquires helical and turn structures upon interaction with the DNA (Vila et al. 2001).

Histone H1 has been described as a general transcriptional repressor because it contributes to chromatin condensation, which limits the access of the transcriptional machinery to DNA. However, recent studies show that linker histones participate in complexes that can either activate or repress specific genes (Zlatanova and Van Holde 1992; Khochbin and Wolffe 1994; Wolffe et al. 1997). These regulatory functions of histone H1 are attributed in some cases to the globular domain and in others to the tail-like domains (Bouvet et al. 1994; Shen and Gorovsky 1996; Lee and Archer 1998; Vermaak et al. 1998; Dou et al. 1999). Understanding the structural properties of the H1 terminal domains may clarify its function in chromatin.

The N-terminal domains of H1 histones have two distinct subregions (Böhm and Mitchel 1985). The distal part is rich in alanine and proline and highly hydrophobic, whereas the region adjacent to the globular domain is highly basic and may be involved in the location and anchoring of the globular domain (Allan et al. 1986).

Here we study the conformational properties of the peptide Ac-EKTPVKKKARKAAGGAKRKTSG-NH_2 (NE-1) that comprises the positively charged region of the N-terminal domain of linker histone subtype H1e. This is the most abundant subtype in many mammalian somatic cells. We show that this region has little structure in aqueous solution, but that it acquires a high degree of α-helical structure in the presence of TFE. In 90% TFE, the peptide is organized in two amphipathic α-helices, separated by a Gly–Gly motif, which allows great freedom to the orientation of the two helical elements. This feature may allow the tracking of the DNA phosphate backbone by the α-helices or simultaneous binding to two nonconsecutive DNA segments.

Results

Circular dichroism analysis

We have studied the peptide Ac-EKTPVKKKARKAAG-GAKRKTSG-NH_2 (NE-1), which corresponds to the positively charged region of the N-terminal domain, immediately adjacent to the globular domain, of mouse histone H1e (residues 15–36). None of the first 14 residues of the protein is positively charged.

In aqueous solution, the CD spectrum of the NE-1 peptide was dominated by the random coil component. Neither the double minimum at 208 nm and 222 nm nor the maximum at 190 nm of the α-helix was observed (Fig. 1A). The mean residue molar ellipticity at 222 nm ($[\theta]_{222}$), taken as diagnostic of helix formation, was negligible in water. However,

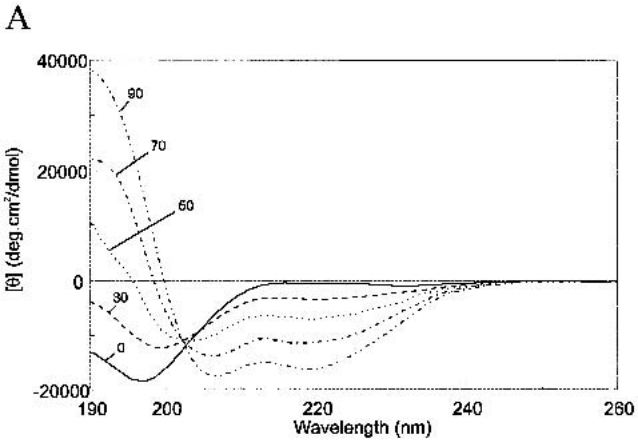

B

% TFE	$[\theta]_{222nm}$	% helix
90	-15324	44
70	-10706	31
50	-6378	18
30	-3174	9
0	-366	1

Fig. 1. TFE-dependent conformational transition of the NE-1 peptide measured by CD. (*A*) Far-UV CD spectra in the presence of various concentrations of TFE in 10 mM NaCl, phosphate buffer 5 mM, pH 3.5 at 20°C. The numbers refer to the TFE concentration in percentage by volume. (*B*) Variation of the mean residue molar ellipticity, [θ] in degrees-centimeter squared per decimole, at 222 nm with added TFE. The percentage of helical structure, calculated as described in Materials and Methods, is also indicated.

the absence of a small positive peak at ~215 nm, a feature characteristic of the random coil, indicated that a small amount of structure was present.

Addition of TFE, which stabilizes peptide secondary structure, increased the α-helical content, as shown by the increase in the negative ellipticity at 222 nm and the change in the shape of the spectrum. The transition between the random coil and the helical structure seems to be a two-state equilibrium, as indicated by the presence of an isodichroic point. The helical content of the peptide as a function of TFE concentration estimated by the method of Chen et al. (1974) is shown in Figure 1. In 50% and 90% TFE solution, the helical populations were 18% and 44%, respectively. The method of Rohl and Baldwin (1997) gave slightly higher values of 21% and 47%, respectively. It should be noted, however, that CD methods provide only a rough estimate of the helical content.

NMR analysis

The NMR spectra were recorded in 50% and 90% TFE at pH 3.5 and 25°C. Figure 2 summarizes all relevant NOE

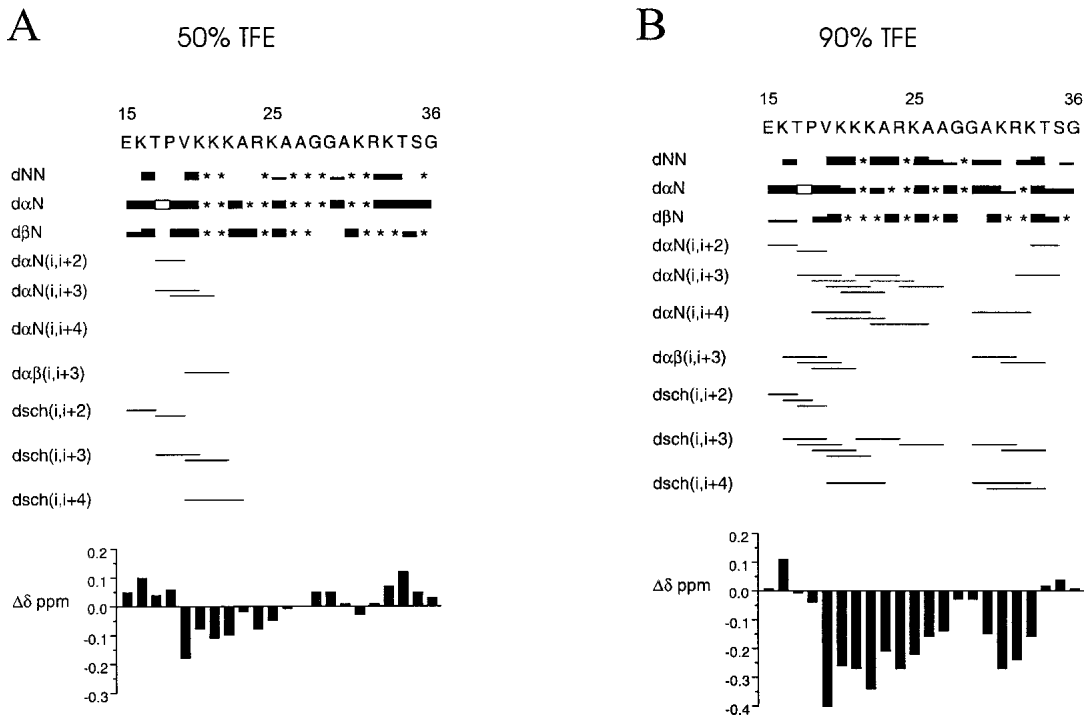

Fig. 2. Summary of the NOE connectivities of NE-1. (*A*) The results in 50% TFE solution and (*B*) in 90% TFE solution are presented (25°C, pH 3.5). The thickness of the lines reflects the intensity of the sequential NOE connectivities, that is, weak, medium, and strong. An asterisk (*) indicates an unobserved NOE connectivity caused by signal overlapping, proximity to the diagonal, or overlapping with the solvent signal. An open box indicates a $d\alpha\delta(i, i + 1)$ NOE connectivity, where $i + 1$ is proline. dsch indicates NOE connectivities involving side chains. The conformational shifts with respect to random coil values, $C_\alpha H$ $\Delta\delta$, are shown as a function of the sequence number (*bottom*).

data for the peptide in 50% and 90% TFE. The figure also shows the plot of the conformational shifts of the $C_\alpha H$ protons, $\Delta\delta = \delta_{observed} - \delta_{random\ coil}$.

The presence of helical conformations was established on the basis of the following criteria: (1) the presence of stretches of nonsequential $\alpha N(i, i + 3)$, $\alpha N(i, i + 4)$, $\alpha\beta(i, i + 3)$, as well as side-chain–side-chain and side-chain–main-chain $(i, i + 3)$ and $(i, i + 4)$ NOE connectivities; (2) strong sequential *NN* NOE connectivities, concomitant with weakened $\alpha N(i, i + 1)$ NOE connectivities; (3) significant up-field shift of the $C_\alpha H$ resonances relative to the random coil values; (4) $^3J_{C_\alpha}H$–NH couplings <5.0 Hz.

In 50% TFE, the NE-1 peptide showed a low α-helical population. In these conditions, the helix may begin at Thr17, with Pro18 in the statistically favored N + 1 position (Richardson and Richardson 1988), and span to Ala26.

In 90% TFE, the helical population increased considerably, and spanned almost the entire peptide, as shown by the presence of numerous $(i, i + 3)$ and $(i, i + 4)$ NOE connectivities, the reinforcement of sequential *NN* NOEs, the up-field shift of the $C_\alpha H$ resonances, and the $^3J_{C_\alpha}H$–NH < 5.0 Hz for residues T17, K20, R24, A26, A27, K31, and K33. All these features are interrupted around the Gly28–Gly29 doublet. This indicates that NE-1 is organized in two α-helical elements separated by the Gly–Gly motif. The N-terminal α-helix (helix N-I) begins at Thr17, as this residue presents a $^3J_{C_\alpha}H$–NH < 5.0 Hz and it is the first involved in an $\alpha N(i, i + 3)$ NOE connectivity. This helical element spans to Ala27, as shown by the abundance of $(i, i + 3)$ and $(i, i + 4)$ NOEs, the negative and large in absolute value $C_\alpha H$ $\Delta\delta$ within the Val19–Ala27 segment, and the $^3J_{C_\alpha}H$–NH coupling constants <5.0 Hz for residues T17, K20, R24, A26, and A27. The fractional helicity of this region was 54%, according to the $C_\alpha H$ $\Delta\delta$.

The C-terminal α-helix (helix N-II) is shorter and somewhat less stable than the N-terminal one, as deduced from its absence in 50% TFE and the slightly lower helical population in 90% TFE (44%). According to the presence of $(i, i + 3)$ and $(i, i + 4)$ NOE connectivities, the helix spans from Ala30 to Thr34, with Gly29, which is involved in an $\alpha N(i, i + 4)$ NOE cross-peak, as N-Cap. This region contains two residues, Lys31 and Lys33, with $^3J_{C_\alpha}H$–NH < 5.0 Hz. The helix may include Ser35, because this residue is involved in an $\alpha N(i, i + 3)$ NOE cross-correlation.

Structure calculations

The structure calculations were performed on the basis of the NOE cross-correlations observed in 90% TFE. A set of

89 distance constraints, composed of 21 sequential and 68 medium-range constraints, was used to calculate the three-dimensional structures of the peptide. A total of 50 structures were generated with the torsion angle dynamics program DYANA (Güntert et al. 1997). The 22 best converged structures were chosen. The global RMS deviation of the backbone atoms of the whole peptide, excluding the first and the last residues, for this set of structures was 0.30 ± 0.09 nm, and the maximum NOE violation was 0.07 nm. Figure 3 shows the superposition of the backbones of the 22 selected structures. The region spanning from Thr17 to Ala27 adopts a well-defined helical structure, as does the region from Ala30 to Thr34. In some structures Ser35 is also included in the C-terminal helix. The calculated structures are highly flexible about the Gly28–Gly29 motif, which results in a wide range of values for the angle defined by the two helical axes. This obliges us to show the set of calculated structures fitted either for the N-terminal helical region (Fig. 4A) or for the C-terminal one (Fig. 4B).

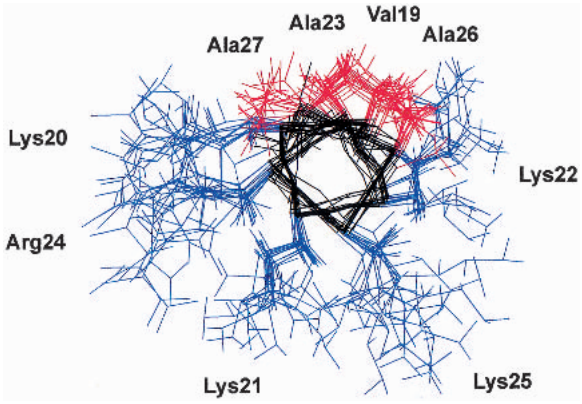

Fig. 4. End view down the helix axis of the 22 best converged structures of helix I of NE-1. The helical region from Val19 to Ala27 is represented. It shows the amphipathic character of the helix, with the positively charged residues on one face of the helix and the hydrophobic residues on the other.

Discussion

Histone H1 terminal domains have little structure in aqueous solution. Secondary-structure inducers promote the formation of turns and helices in the C-terminal domain (Clark et al. 1988; Hill et al. 1989; Suzuki et al. 1993; Vila et al. 2000). It has been shown that interaction with the DNA induces helical and turn structures in an H1 C-terminal peptide (Vila et al. 2001). However, very little is known so far regarding the N-terminal domain functional and structural properties.

We have studied the structure of the NE-1 peptide, which corresponds to the charged region of the N-terminal domain of histone H1e, by CD and ^{1}H-NMR. In aqueous solution, NE-1 behaved as a mainly unstructured peptide. Addition of TFE resulted in a substantial increase of the helical content. In 90% TFE, the peptide was structured in two α-helices spanning from Thr17 to Ala27 (helix N-I) and from Gly29 to Thr34 (helix N-II), with fractional helicities of 54% and 44%, respectively. These results, calculated from the upfield shifts of the $C_\alpha H$ δ values, are in good agreement with the average value of 44% obtained by CD for the entire peptide. The presence of an $\alpha N(i, i+3)$ NOE cross-peak involving Ser35 indicates that this residue may also be in-

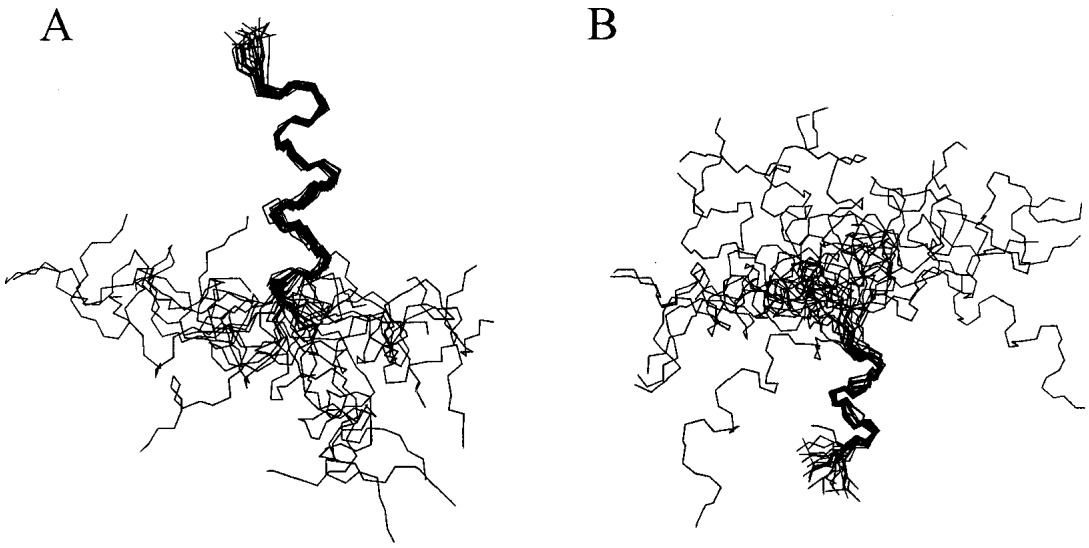

Fig. 3. Superposition of the backbone of the 22 NE-1 peptide best converged structures calculated by the torsion angle dynamics program DYANA (Güntert et al. 1997) on the basis of the distance constraints derived from observed NOE cross-correlations in 90% TFE solution. (*A*) The 22 structures fitted at the N-terminal helix. (*B*) The 22 structures fitted at the C-terminal helix.

cluded in helix N-II, as in some of the calculated structures. The lack of defined secondary structure when NE-1 is studied in the absence of TFE is correctly predicted by the helix prediction program AGADIR, which has been parameterized on the basis of peptide conformations in aqueous solution (Muñoz and Serrano 1994). When the method of Chou and Fasman (1974), which is based on protein data, is used, the two α-helical elements are correctly predicted.

TFE stabilizes helical and turn structures (Buck 1998), revealing the conformational biases of the primary sequence. Although TFE has been extensively used, the mechanism by which it affects the polypeptide structure is not fully understood. Enhancement of hydrogen bonding, disruption of the water structure, and preferential solvation of certain groups of the polypeptide chain have been suggested as possible explanations. It has also been argued that TFE could associate with the hydrophobic surface of amphipathic helices and mimic a dehydrated environment (Buck 1998). The electrostatic repulsion between the positively charged residues in the amphipathic helices could explain the unusually high TFE concentration necessary to stabilize histone H1 helices (Walters and Kaiser 1985; Clark et al. 1988; Hill et al. 1989; Johnson et al. 1994; Vila et al. 2000, 2001).

Both helical elements in the N-terminal domain of H1e have a marked amphipathic character, with all the basic residues on one face of the helices and the apolar residues on the other (Fig. 4). The mean helical hydrophobic moments, $\langle \mu_H \rangle$ (Eisenberg et al. 1982, 1984), for helices N-I (residues Thr17–Ala27) and N-II (residues Gly29–Thr34) were 0.33 and 0.23, respectively. These values are to be compared with $\langle \mu_H \rangle = 0.53$ for the highly amphipathic helix $(KKLL)_3$. The positively charged amphipathic α-helices have been described as DNA-binding motifs. Our results indicate that the positively charged region of the N-terminal domain adopts α-helical structure upon binding to the DNA, as proposed for some of the sequences of the C-terminal domain (Clark et al. 1988; Hill et al. 1989; Vila et al. 2000, 2001).

Helix N-II surpasses the limit between the N-terminal and the globular domains defined by trypsin cutting at Lys33. This indicates that the structural limit between the domains is the helix-disruptive motif Pro37–Pro38, which is immediately adjacent to helix I of the globular domain. Figure 5A shows a model structure of the N-terminal peptide of H1e connected to the NMR structure of the globular domain of chicken histone H1 (Cerf et al. 1993). The proximity of the helix–Gly–Gly–helix motif to the globular domain and its high positive charge density support the view that this region is involved in the location and anchoring of the globular domain to the nucleosome (Allan et al. 1986).

Both N-terminal domain helical elements contain a triplet of basic residues. Basic triplets are not frequent in somatic H1 subtypes, but they are more common in non- sequence-specific DNA-binding proteins with high affinity for the DNA, such as sperm linker histones and protamines (Subirana 1990). The triplets of basic residues probably confer a high DNA-binding affinity to the proximal region of the N-terminal domain. The inducible character of the helical elements of the terminal domains may prevent the highly charged N-terminal region from strongly binding to DNA before the globular domain is correctly positioned on the nucleosome.

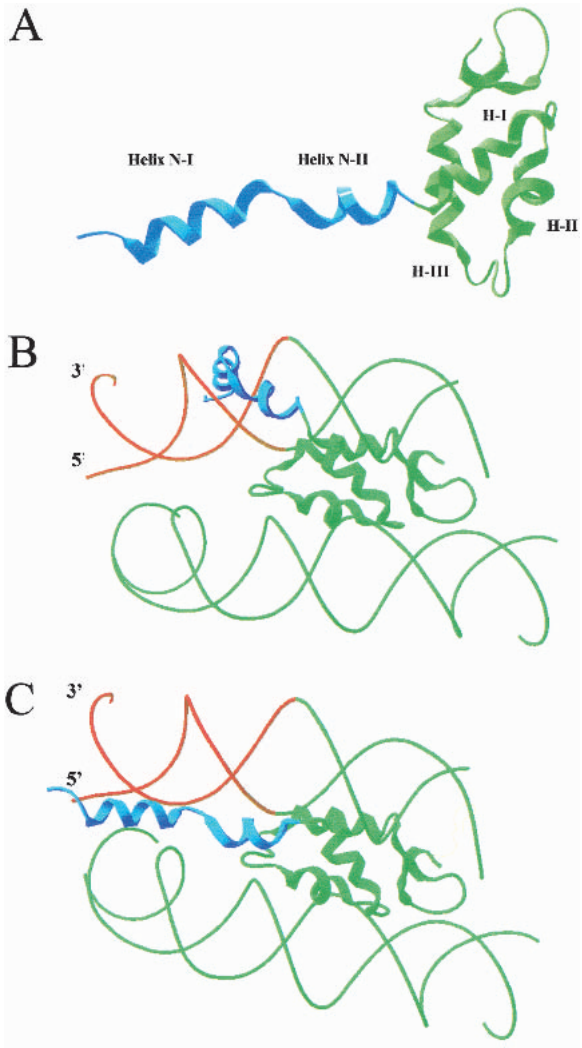

Fig. 5. Model of the binding of the N-terminal domain of histone H1e to the nucleosome. (*A*) Model structure of the connection of the N-terminal and globular domains. The NMR structure of the folded N-terminal domain NE-1 peptide is shown connected to the NMR structure of the globular domain of chicken histone H1 globular domain. (*B*) Representation of a possible location of the N-terminal domain bound to linker DNA. (*C*) Representation of the N-terminal domain bound to chromatosomal and linker DNA. The chromatosomal DNA is in green, the linker DNA is in red, the histone H1 N-terminal domain is in blue, and the globular domain is in green. The globular domain is located according to the model of Zhou et al. (1998).

The two α-helical elements in the N-terminal domain are separated by a Gly–Gly motif. The Gly–Gly doublet behaves as a flexible linker between the helical elements. The Gly–Gly doublet is conserved at equivalent positions in many vertebrate H1 subtypes (Sullivan et al. 2000). A Gly–Gly motif is found in the porins of *Escherichia coli* and other bacterial species (Jeanteur et al. 1991). The motif confers flexibility to the third loop of the protein, which appears to have functional implications (Van Gelder et al. 1997). Another example of structural flexibility associated with a Gly sequence is that of the calmodulin-related TCH2 protein from *Arabidopsis*. Its overall structure consists of two globular domains separated by a flexible linker region that contains a $(Gly)_4$ motif (Khan et al. 1997).

Figure 5 (B and C) shows a representation of the binding of the N-terminal domain to the DNA in chromatin. Helix III of the globular domain interacts at one terminus of the chromatosome, according to the model of Zhou et al. (1998). This places the N-terminal domain near the linker DNA. The wide range of possible orientations of the two N-terminal α-helices allowed by the Gly–Gly motif could facilitate the tracking of the phosphate backbone of the linker DNA by the helical elements (Fig. 5B) or the simultaneous binding of nucleosomal and linker DNA (Fig. 5C).

Materials and methods

Peptide synthesis

The peptide Ac-EKTPVKKKARKAAGGAKRKTSG-NH_2 (NE-1) was synthesized by standard methods (DiverDrugs, Barcelona, Spain). Peptide homogeneity was determined by HPLC on Kromasil C8. The peptide composition was confirmed by amino acid analysis, and the molecular mass was checked by mass spectrometry. The sequence of the peptide corresponds to residues 15 to 36 at the N terminus of mouse histone H1e. It presents two substitutions in the rat, at positions 19 (Val → Ile) and 34 (Thr → Ala); and three in humans, at positions 26 (Ala → Ser), 29 (Gly → Ala), and 34 (Thr → Ala). The peptide was acetylated and amidated to remove the dipole destabilization effect.

Circular dichroism spectroscopy

Samples for circular dichroism spectroscopy were 2.85×10^{-5} M in the peptide and 5 mM in sodium phosphate buffer, 10 mM NaCl at pH 3.5. Samples in aqueous and mixed solvent with different ratios (v/v) of trifluoroethanol/H_2O were prepared. Spectra were obtained on a Jasco J-715 CD spectrometer in 1-mm cells at 20°C. The results are expressed as mean residue molar ellipticities, [θ]. The helical content was estimated from the ellipticity value at 222 nm, $[\theta]_{222}$, according to the empirical equation of Chen et al. (1974):

$$\%\text{helical content} = 100\,([\theta]_{222}/-39500 \times (1 - 2.57/n)),$$

where n is the number of peptide bonds.

The mean helix content, f_H, was also calculated according to Rohl and Baldwin (1997):

$$f_H = (\theta_{222} - \theta_C)/(\theta_H - \theta_C);$$

were θ_C and θ_H are given by the following expressions:

$$\theta_C = 2220 - 53T$$

$$\theta_H = (-44000 + 250T)(1 - 3/N_r)$$

where T is the temperature in degrees Celsius and N_r is the chain length in residues.

^{1}H NMR spectroscopy

Samples were routinely prepared as ~2.6 mM solutions of the peptide in H_2O, 5 mM phosphate buffer, 10 mM NaCl, and the presence of either 50% or 90% deuterated TFE. The pH was adjusted to 3.5 with minimal amounts of HCl or NaOH in water. Spectra were obtained at 25°C.

Spectra were recorded in a Bruker AMX-600 spectrometer as described previously (Vila et al. 2000). The assignments of the ^{1}H-NMR spectra of the peptide in the presence of different concentrations of trifluoroethanol were performed by standard two-dimensional sequence-specific methods (Wüthrich et al. 1984; Wüthrich 1986).

The helix populations were quantified on the basis of the upfield shifts of the $C_\alpha H$ δ values upon helix formation, according to Jiménez et al. (1993). The average helical population per residue was calculated by dividing the average conformational shift, $\Delta\delta = \Sigma(\delta_{i_{obs}} - \delta_{i_{RC}})/n$, by the shift corresponding to 100% helix formation. Random coil values, δ_{RC}, were those given by Wüthrich (1986), except for Thr17, which was that given for amino acids followed by Pro (Wishart et al. 1995). A value of −0.39 ppm was used as the shift for 100% helix formation (Wishart et al. 1991). The helical length, n, was determined on the basis of NOE cross-peaks, couplings $^3J_{C_\alpha}$H–NH < 5.0 Hz, and conformational shifts, and confirmed by structure calculations.

$^3J_{C_\alpha}$H–NH coupling constants for nonoverlapping signals were determined by analyzing TOCSY spectra using the method of Stonehouse and Keeler (1995).

Structure calculations

Peptide structures were calculated with the program DYANA (Güntert et al. 1997). Distance constraints were derived from the 150-msec NOESY spectrum acquired in 90% TFE at 25°C and pH 3.5. The intensities of the observed NOEs were evaluated qualitatively and translated into upper-limit distance constraints according to the following criteria: strong NOEs were set to distances lower than 0.3 nm; medium, lower than 0.35 nm, and weak, lower than 0.45 nm. Pseudo-atom corrections were set to the sum of the van der Waals radii. ϕ angles for those residues with $^3J_{C_\alpha}$H–NH < 5.0 Hz (T3, K6, R10, A12, A13, K17, and K19) were restricted to the range −90° to −30°. The ϕ angles of the rest of the residues except for Gly were constrained to the range −180° to 0°.

Acknowledgments

This study was supported by the Ministerio de Educación y Cultura, (DGICYT, PB98-0896), the Generalitat de Catalunya (2000SGR-00065), and the EU (CEE B104–97–2086).

The publication costs of this article were defrayed in part by payment of page charges. This article must therefore be hereby

marked "advertisement" in accordance with 18 USC section 1734 solely to indicate this fact.

References

Allan, J., Mitchell, T. Harborne, N., Böhm, L., and Crane-Robinson, C. 1986. Roles of H1 domains in determining higher order chromatin structure and H1 location. *J. Mol. Biol.* **187:** 591–601.

Böhm, L. and Mitchell, T.C. 1985. Sequence conservation in the N-terminal domain of histone H1. *FEBS Lett.* **193:** 1–4.

Bouvet, P., Dimitrov, S., and Wolffe, A.P. 1994. Specific regulation of *Xenopus* chromosomal 5S rRNA gene transcription in vivo by histone H1. *Genes & Dev.* **8:** 1147–1159.

Buck, M. 1998. Trifluoroethanol and colleagues: Cosolvents come of age. Recent studies with peptides and proteins. *Q. Rev. Biophys.* **31:** 297–355.

Cerf, C., Lippens, G., Muyldermans, S., Sergers, A., Ramakrishnan, V., Wodak, S.J., Hallenga, K., and Wyns, L. 1993. Homo- and heteronuclear two-dimensional NMR studies of the globular domain of histone H1: Sequential assignment and secondary structure. *Biochemistry* **32:** 11345–11351.

Chen, Y.H., Yang, J.T., and Chau, K.H. 1974. Determination of the helix and β-form proteins in aqueous solution by circular dichroism. *Biochemistry* **13:** 3350–3359.

Chou, P.Y. and Fasman, G.D. 1974. Prediction of protein conformation. *Biochemistry* **13:** 222–245.

Clark, D.J., Hill, C.S., Martin, S.R., and Thomas, J.O. 1988. α-Helix in the carboxy-terminal domain of histones H1 and H5. *EMBO J.* **7:** 69–75.

Clore, G.M., Gronenborn, A.M., Nilges, M., Sukumaran, D.K., and Zarbock, J. 1987. The polypeptide fold of the globular domain of histone H5 in solution. A study using nuclear magnetic resonance, distance geometry and restrained molecular dynamics. *EMBO J.* **6:** 1833–1842.

Dou, Y., Mizzen, C.A., Abrams, M., Allis, C.D., and Gorovsky, M.A. 1999. Phosphorylation of linker histone H1 regulates gene expression in vivo by mimicking H1 removal. *Mol. Cell* **4:** 641–647.

Eisenberg, D., Weiss, R.M., and Terwilliger, T.C. 1982. The helical hydrophobic moment: A measure of the amphiphilicity of a helix. *Nature* **299:** 371–374.

———. 1984. The hydrophobic moment detects periodicity in protein hydrophobicity. *Proc. Natl. Acad. Sci.* **81:** 140–144.

Güntert, P., Mumenthaler, C., and Wuthrich, K. 1997. Torsion angle dynamics for NMR structure calculation with the new program DYANA. *J. Mol. Biol.* **273:** 283–298.

Hartman, P.G., Chapman, G.E., Moss, T., and Bradbury, E.M. 1977. Studies on the role and mode of operation of the very-lysine-rich histone H1 in eukaryotic chromatin: The three structural regions of the histone H1 molecule. *Eur. J. Biochem.* **77:** 45–51.

Hill, C.S., Martin, S.R., and Thomas, J.O. 1989. A stable α-helical element in the carboxy-terminal domain of free and chromatin-bound histone H1 from sea urchin sperm. *EMBO J.* **8:** 2591–2599.

Jeanteur, D., Lakey, J.H., and Pattus, F. 1991. The bacterial porin superfamily: Sequence alignment and structure prediction. *Mol. Microbiol.* **5:** 2153–2164.

Jiménez, M.A., Bruix, M, González, C., Blanco, F.J., Nieto, J.L., Herranz, J., and Rico, M. 1993. CD and ^{1}H-NMR studies on the conformational properties of peptide fragments from the C-terminal domain of thermolysin. *Eur. J. Biochem.* **211:** 569–581.

Johnson, N.P., Lindstrom, J., Baase, W.A., and von Hippel, P.H. 1994. Double-stranded DNA templates can induce α-helical conformation in peptides containing lysine and alanine: Functional implication for leucine zipper and helix-loop-helix transcription factors. *Proc. Natl. Acad. Sci.* **91:** 4840–4844.

Khan, A.R., Johnson, K.A., Braam, J., and James, M.N.G. 1997. Comparative modeling of the three-dimensional structure of the calmodulin-related TCH2 protein from *Arabidopsis*. *Prot. Struc. Func. Genet.* **27:** 144–153.

Khochbin, S. and Wolffe, A.P. 1994. Developmentally regulated expression of linker-histone variants in vertebrates. *Eur. J. Biochem.* **225:** 501–510.

Lee, H.L. and Archer, T.K. 1998. Prolonged glucocorticoid exposure dephosphorylates histone H1 and inactivates the MMTV promoter. *EMBO J.* **17:** 1454–1466.

Muñoz, V. and Serrano, L. 1994. Elucidating the folding problem of helical peptides using empirical parameters. *Nat. Struct. Biol.* **1:** 399–409.

Ramakrishnan, V., Finch, J.T., Graziano, V., Lee, P.L., and Sweet, R.M. 1993. Crystal structure of globular domain of histone H5 and its implications for nucleosome binding. *Nature* **362:** 219–223.

Richardson, J.S. and Richardson, D.C. 1988. Amino acid preferences for specific locations of the ends of α helices. *Science* **240:** 1648–1652.

Rohl, C.A. and Baldwin, R.L. 1997. Comparison of NH exchange and circular dichroism as techniques for measuring the parameters of helix-coil transition in peptides. *Biochemistry* **36:** 8435–8442.

Shen, X. and Gorovsky, M.A. 1996. Linker histone H1 regulates specific gene expression but not global transcription in vivo. *Cell* **86:** 475–483.

Stonehouse, J. and Keeler, J. 1995. A convenient and accurate method for the measurement of the values of spin-spin coupling constants. *J. Magn. Reson. (Series A)* **112:** 43–57.

Subirana, J.A. 1990. Analysis of the charge distribution in the C-terminal region of histone H1 as related to its interaction with DNA. *Biopolymers* **29:**1351–1357.

Sullivan, S.A., Aravind, L., Makalowska, I., Baxevanis, A.D., and Landsman, D. 2000. The histone database: A comprehensive WWW resouce for histones and histone fold-containing proteins. *Nucleic Acids Res.* **28:** 323–325.

Suzuki, M., Gerstein, M., and Johnson, T. 1993. An NMR study on DNA-binding SPKK motif and a model for its interaction with DNA. *Protein Eng.* **6:** 565–574.

Van Gelder, P., Saint, N., van Boxtel, R., Rosenbusch, J.P., and Tommassen, J. 1997. Pore functioning of outer membrane protein PhoE of *Escherichia coli*: Mutagenesis of the constriction loop L3. *Protein Eng.* **10:** 699–706.

Vermaak, D., Steinbach, O.C., Dimitrov, S., Rupp, R.A.W., and Wolffe, A.P. 1998. The globular domain of histone H1 is sufficient to direct specific gene repression in early *Xenopus* embryos. *Curr. Biol.* **8:** 533–536.

Vila, R., Ponte, I., Jiménez, M.A., Rico, M., and Suau, P. 2000. A helix-turn motif in the C-terminal domain of histone H1. *Protein Sci.* **9:** 627–636.

Vila, R., Ponte, I., Collado, M., Arrondo, J.L.R., and Suau, P. 2001. Induction of secondary structure in a COOH-terminal peptide of histone H1 by interaction with the DNA: An infrared spectroscopy study. *J. Biol. Chem.* **276:** 30898–30903.

Walters, L. and Kaiser, E.T. 1985. Design of DNA-binding peptides: Stabilization of α-helical structure by DNA. *J. Am. Chem. Soc.* **107:** 6422–6424.

Wishart, D.S., Sykes, B.D., and Richards, F.M. 1991. Relationship between nuclear magnetic resonance chemical shift and secondary structure. *J. Mol. Biol.* **222:** 311–333.

Wishart, D.S., Brigam, C.G., Holm, A., Hodges, R.S., and Sykes, B.D. 1995. ^{1}H, ^{13}C and ^{15}N random coil NMR chemical shifts of the common amino acids. I. Investigations of the nearest-neighbor effects. *J. Biomol. NMR* **5:** 67–81.

Wolffe, A.P., Khochbin, P.S., and Dimitrov, S. 1997. What do linker histones do in chromatin? *BioEssays* **19:** 249–255.

Wüthrich, K. 1986. *NMR of protein and nucleic acids*. John Wiley, New York.

Wüthrich, K., Billeter, M., and Braun, W. 1984. Polypeptide secondary structure determination by nuclear magnetic resonance observation of short proton-proton distances. *J. Mol. Biol.* **180:** 715–740.

Zhou, Y.-B., Gerchman, S.E., Ramakrishnan, V., Travers, A., and Muyldermans, S. 1998. Position and orientation of the globular domain of linker histone H5 on the nucleosome. *Nature* **395:** 402–405.

Zlatanova, J. and van Holde, K. 1992. Histone H1 and transcription: Still an enigma? *J. Cell Sci.* **103:** 889–895.